An Electronic Directional Coupler

The transformers and stepped-gain attenuator required for a classical directional coupler have been successfully integrated onto a single S-Band MMIC that features adjustable coupling over a 30 dB range

By Mitchell Shifrin, Christopher Lyons
Wes Grammer and Peter Katzin
Hittite Microwave Corporation

Directional couplers are principal elements in beam-forming networks for phased-array antennas in such applications as monopulse radar. In systems that use an array of monolithic transmit and receive (T/R) modules, a coupler in MMIC form could be integrated in the module, saving space and lowering overall cost. This paper describes such a monolithic directional coupler.

Figure 1 illustrates the functions of the coupler in a monopulse system. In transmit mode, the coupler must pass the exciter signal with minimum loss and phase distortion. In receive mode, the coupled port amplitude must be controllable over a broad range without affecting other coupler parameters such as directivity and isolation. The variable attenuator shown in the sum channel is another element in the beam forming network. It must have minimum phase change with attenuation and good linearity. This article presents the design and measured data for both components.

The programmable directional coupler MMIC consists of two elements: a lumped-element, broadband coupler with a novel planar transformer layout and a variable-gain amplifier, adjustable over a ±15 dB range in 30 linear steps. The variable attenuator MMIC is digitally programmable in 1 dB increments, with 5 bits (31 dB) of range. Both MMICs include compensation networks to minimize the insertion phase variation over the range of settings.

Lumped-element coupler

GaAs MMIC power dividers and couplers have been demonstrated using lumped-element or distributed techniques [1-4]. However, these designs are prohibitively large at S-band and do not possess the low through insertion loss and good directivity needed in a programmable coupler application. One alternative is a lumped-element coupler made with two identical, high turns-ratio transformers, as shown in Figure 2. Couplers of this type are used widely at low RF frequencies. The capacitors C_1 and C_2 compensate for the interwinding parasitic capacitance of the transformers, greatly improving the coupler directivity. The L-C network in the through path linearizes the phase response and improves port match over the band of interest.

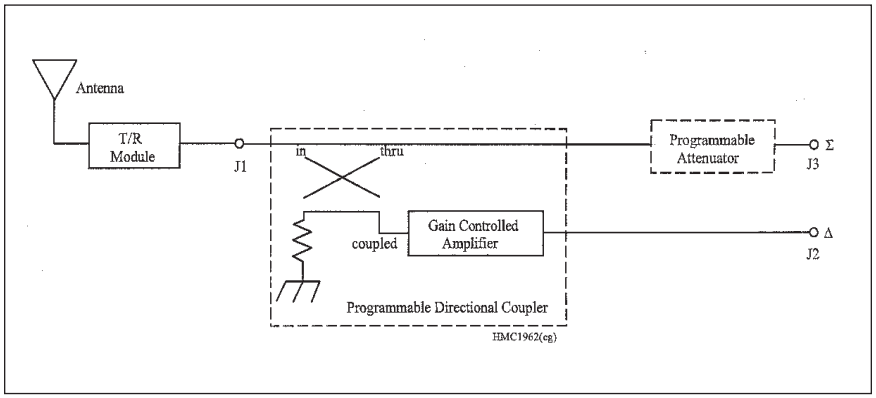

■ **Figure 1. System block diagram, programmable coupler and attenuator.**

The layout in Figure 3 was devised to construct the transformers in planar MMIC form. The secondary winding is a single spiral-wound coil, interwoven with four parallel-connected loops that form the primary. Both windings are air-bridged over most of their lengths to minimize capacitive coupling and loss. The design yields a coupling factor

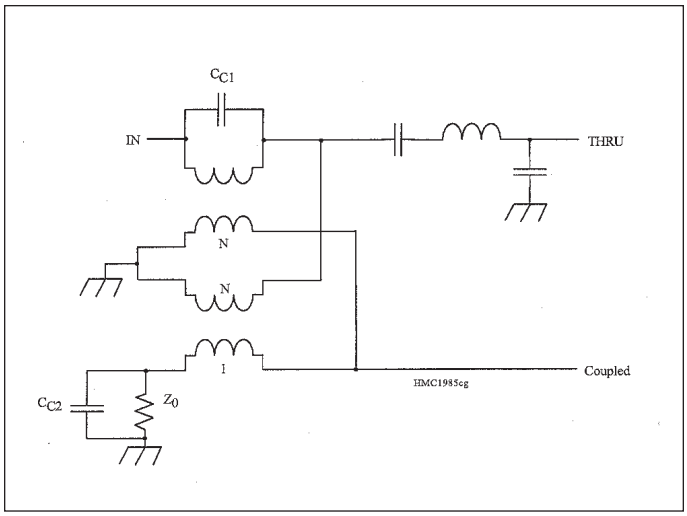

■ **Figure 2. Circuit diagram, lumped-element MMIC coupler.**

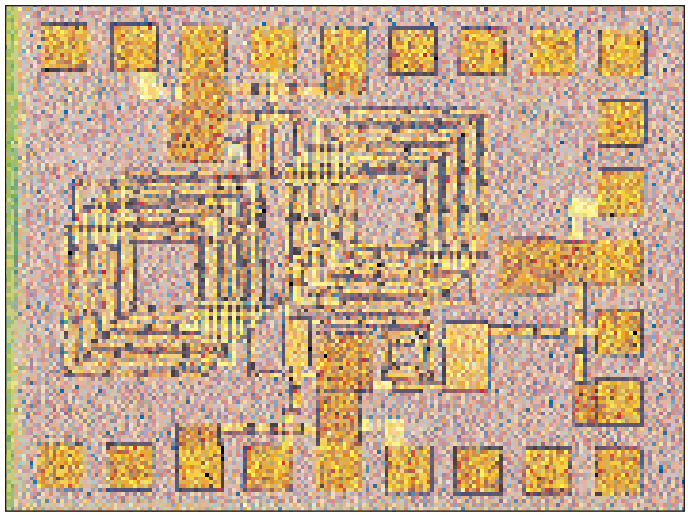

■ **Figure 3. Layout of the coupler test cell.**

K = 0.6, determined from a calculation of the self and mutual inductance of the coils using quasi-static approximations. The total size of the coupler test cell is 1000 × 1300 μm^2.

Variable-gain amplifier

Figure 4 shows the circuit diagram of the amplifier design, including bias networks. A two-stage common-source configuration is used, with lossy interstage and port matching networks to give a flat, broadband gain response and low VSWR. Both stages are biased at I_{DSS}, to eliminate the need for gate bias. The first stage consists of five parallel dual-gate MESFETs, with peripheries scaled in ascending binary order. The second gate functions as a control bit, selectively enabling or disabling a given device. Thus, the composite FET has a transconductance g_m (and hence a gain response) in linear proportion to the binary control inputs.

To compensate for a slight shift in the insertion phase response vs. gain, a small amount of shunt capacitance is added progressively at the lower gain settings. The second stage also uses a dual-gate FET, in this case, to improve isolation of the output load from the variable-gain stage.

The layout of the variable-gain amplifier, configured as an individual test cell, is shown in Figure 5. A Triquint 1 micron process with dielectric vias was used for device fabrication. The cell measures 1.0 × 1.3 mm from the outside edge of the bonding pads.

Integrated coupler/amplifier

The integrated programmable coupler layout is shown in Figure 6. A small capacitance added at the amplifier input compensates for the inductance of the line connecting to the lumped-element coupler. Relocating some of the bias network components makes the design more compact. Otherwise, the amplifier layout is identical to the test cell described earlier. Overall, the cell measures 1.75 × 1.45 mm, including the bonding pads.

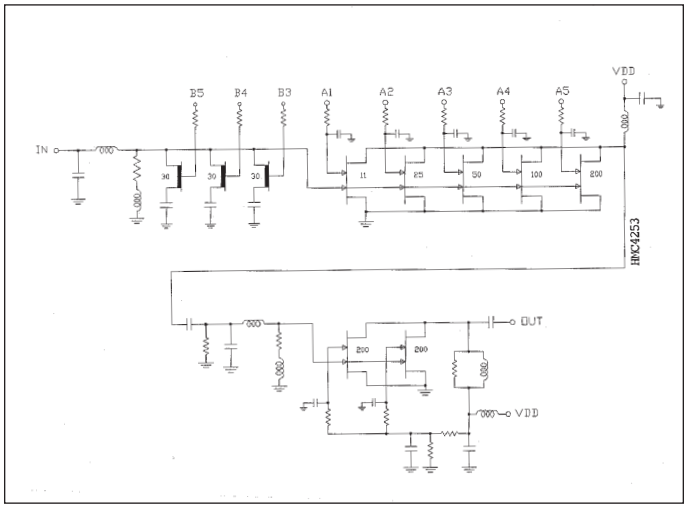

■ **Figure 4. Circuit diagram of the variable-gain amplifier.**

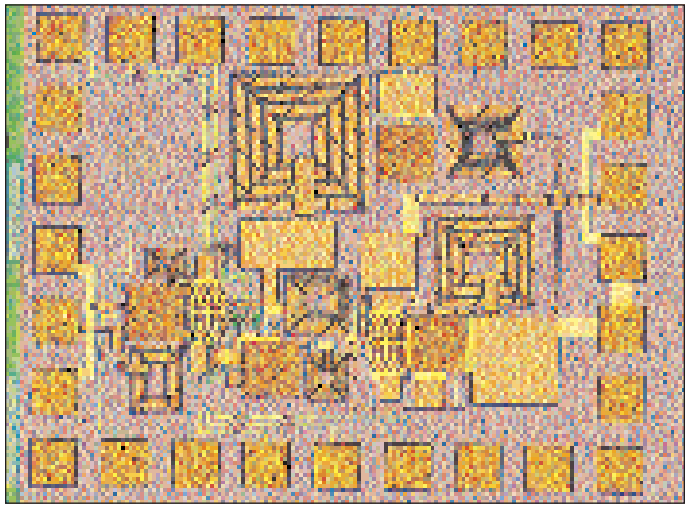

■ **Figure 5. Layout of the amplifier MMIC test cell.**

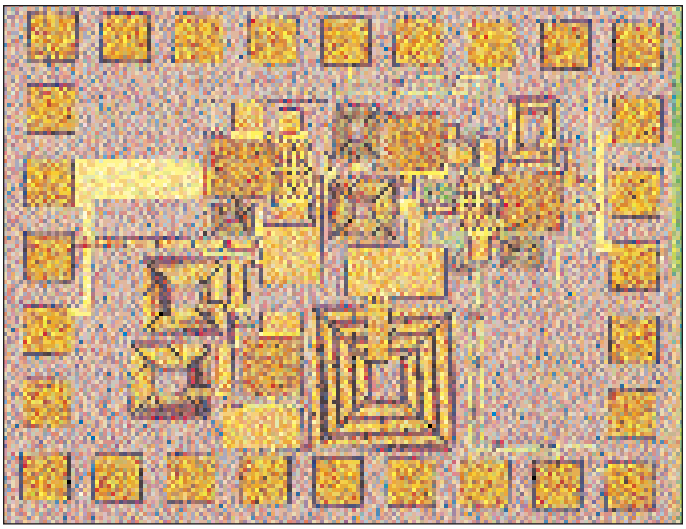

■ **Figure 6. Layout of programmable directional coupler MMIC.**

The RF input and output through ports are on the top and left sides, respectively. The coupled port output is on the right side, and the bottom row of pads are for setting the gain of the coupled signal and for drain bias. Grounded pads on either side of the RF inputs allow wafer probe testing.

Variable attenuator

Figure 7 shows the circuit diagram of the passive 5-bit digital attenuator. The topology uses cascaded sections of 4, 8, 1, 2 and 16 dB, fabricated with MESFET switches and fixed resistors. In the 1 and 2 dB sections, a shunt resistor is switched in to give the appropriate attenuation. Degradation in the match at each port is not severe enough to require a more elaborate circuit, and the OFF state through loss is very low. The 4 and 8 dB sections are elementary pi attenuators, and use a pair of shunt FETs with a single series FET, switched in complementary fashion. The 16 dB stage is merely a cascade of two 8 dB stages. Prior analysis had revealed this configuration would outperform a single-stage design. The series inductors and shunt capacitors included within the attenuator sections were added to equalize the insertion phase in the ON and OFF states. Additional inductance was included between stages to improve the OFF-state match.

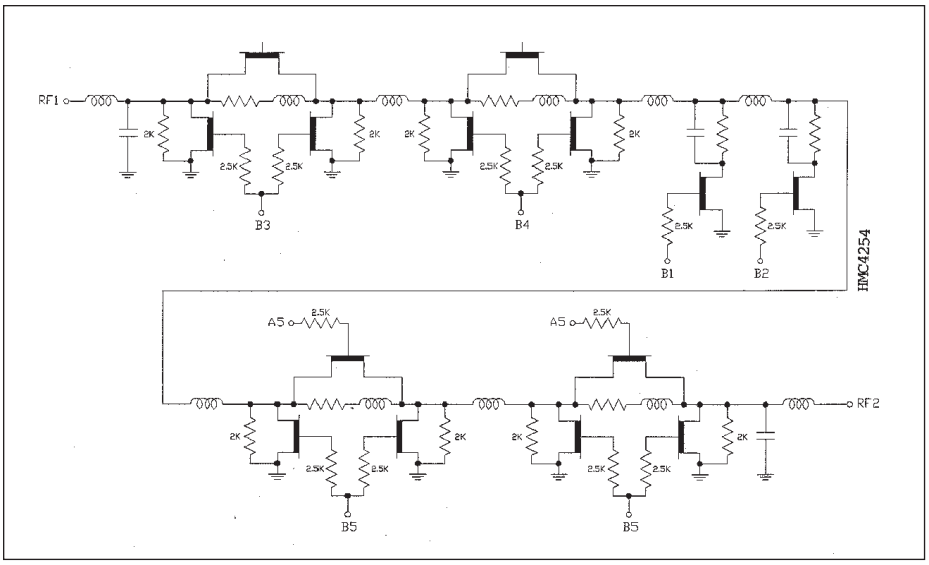

■ **Figure 7. Circuit diagram of the variable attenuator.**

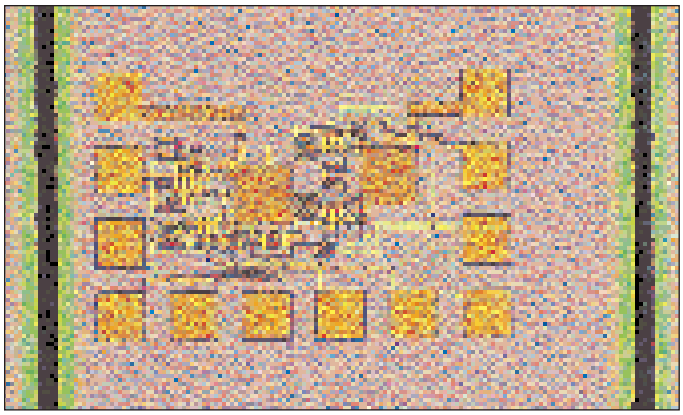

■ **Figure 8. Layout of the variable attenuator MMIC.**

The attenuator circuit was realized in MMIC form using a 1 micron Triquint process with substrate vias. A low-inductance ground path was important in reducing the amount of added reactance needed for phase compensation. Thin-film nichrome (NiCr) resistors are used to insure accuracy, stability and good yields for all critical values. The layout of the attenuator MMIC is shown in Figure 8.

Measurements

The variable attenuator and programmable coupler MMICs were measured on-wafer from 2.5-5.0 GHz using a Hewlett-Packard 8510B network analyzer. In addition, a test fixture containing the MMICs in the configuration of Figure 1 (minus the T/R module) was assembled and measured.

Figure 9 shows the measured through loss of the attenuator for all 32 states, and a plot of the insertion phase, both normalized to the minimum loss ("0 dB") state. The amplitude response is monatonic and flat, with a slight slope at the higher-loss states. The peak-to-peak phase change (all states) is –7°, worst-case, with a computed maximum RMS phase error of less than 3°. Finally, the minimum loss of the attenuator averages around 6.5 dB, with about a ±0.2 dB variation across the band.

The through loss, coupling and isolation of the lumped-element coupler test cell are plotted in Figure 10. The

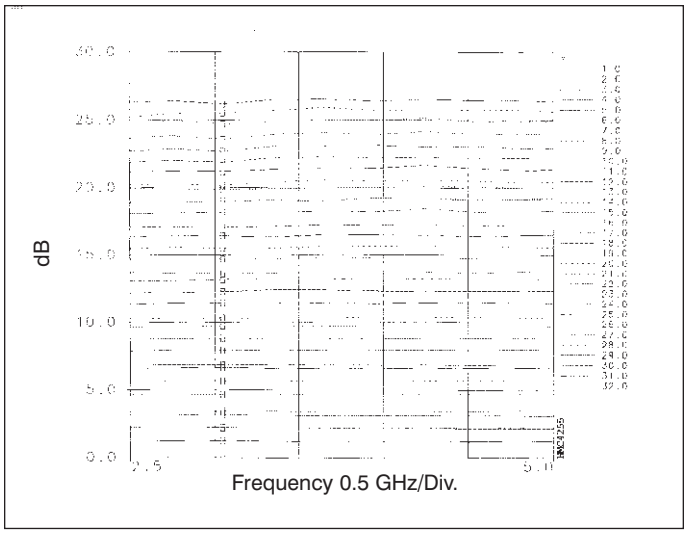

■ **Figure 9a. Measured response of the variable attenuator MMIC: magnitude (dB), normalized.**

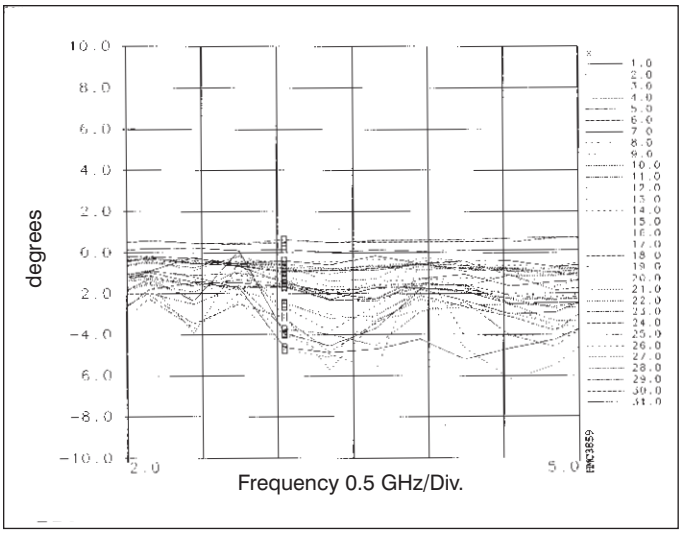

■ **Figure 9b. Measured response of the variable attenuator MMIC: phase (deg.) normalized.**

through loss is low, and the coupling is broad and flat at –15 dB. However, the directivity is much lower than that predicted in our simulations (>20 dB). The reason for this is may be due to unintended coupling between the two transformers, an effect that was not modeled.

Lastly, the measured coupled port insertion loss of the programmable coupler chip is shown in Figure 11(a) for all 32 gain states of the amplifier. Because the scaling of the voltage gain with setting is linear, the responses appear exponential on a dB scale. With a predicted gain of ±15 dB, the results are reasonably close to those predicted in the design simulations.

In Figure 11(b), the phase deviation, (normalized to the highest gain state) shows a fairly large peak error for the lowest 3-4 states, reducing the useable dynamic range by about half. Further improvement in the model used for the segmented dual-gate device in the first amplifier stage

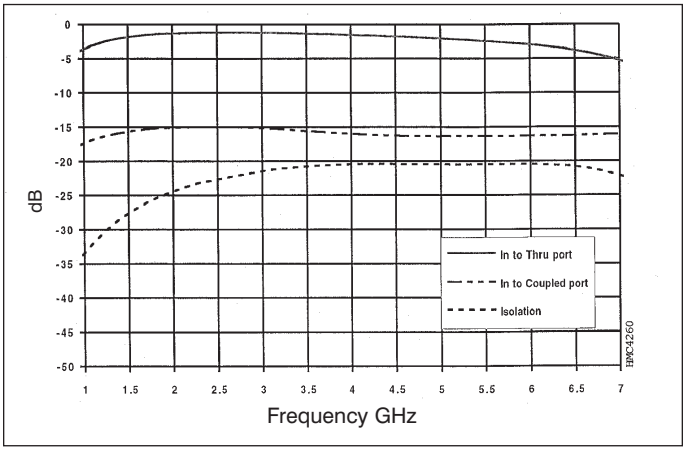

■ **Figure 10. MMIC coupler response.**

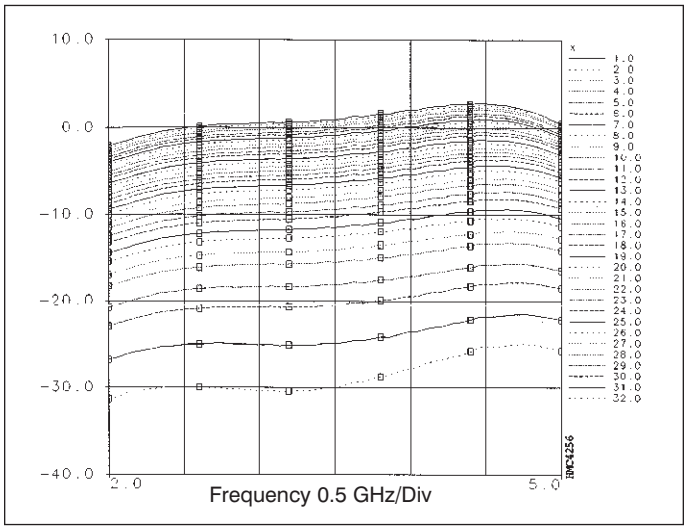

■ **Figure 11a. Measured response of the programmable directional coupler: magnitude (dB).**

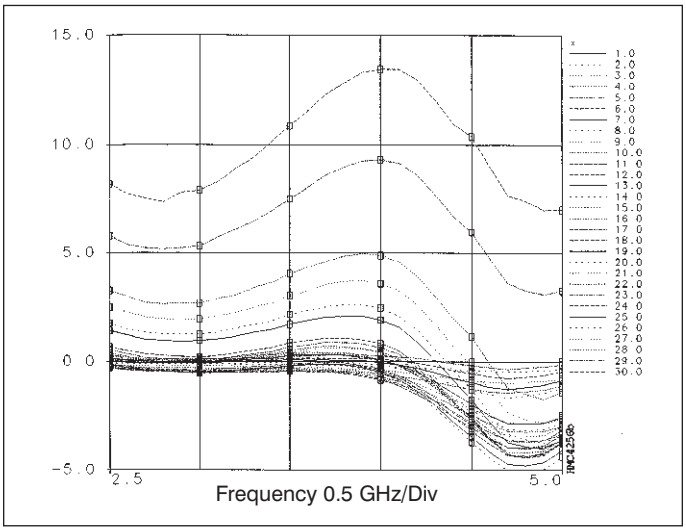

■ **Figure 11b. Measured response of the programmable directional coupler: phase (deg.), normalized, two lowest gain states excluded.**

may improve the phase matching at lower gain settings.

Conclusion

The programmable directional coupler MMIC, suitable for use in phased-array antenna beam-forming networks, has broad bandwidth, low insertion loss and a broad range of programmable coupling ratios. The companion programmable attenuator MMIC has low RMS insertion phase variation. Further work is needed to improve coupled directivity and amplifier gain state phase tracking.

Acknowledgments

This work was supported in part by Rome Laboratory/Electromagnetics Directorate (RL/ERAS), Hanscom Air Force Base, MA, 01731-5000. This paper was derived from the authors' presentation at the 1996 GOMAC Conference entitled "An active monolithic programmable directional coupler for phased-array radars." ■

References

1. R.E. Neidert, S.C. Binari, "mm-Wave Passive Components for Monolithic Circuits," *Microwave Journal*, April 1984, pp. 103-120.

2. W. Beckwith and J. Staudinger, "Wide Bandwidth Monolithic Power Dividers," *Microwave Journal,* February 1989, pp. 150-160.

3. J. Putnam and R. Puente, "A Monolithic Image-Rejection Mixer on GaAs Using Lumped Elements," *Microwave Journal*, November 1987, pp. 107-116.

4. G.E. Brehm and R.L. Lehmann, "Monolithic GaAs Lange Coupler at X-band," *IEEE Trans. on ED*, Vol. ED-28, No. 2, February 1981, pp. 217-218.

Hittite Microwave Corp. can be reached by telephone at (617) 933-7267.

Mitchell B. Shifrin received B.S. degrees in electrical and computer engineering and in applied mathematics and engineering physics from the University of Wisconsin, Madison and an M.S. degree in electrical engineering from the University of Massachusetts. He is engaged in the design of novel MMIC products.

Christopher Lyons received his B.S. degree in electrical engineering from the University of Lowell, Massachusetts in 1982. He is responsible for MMIC assemblies and frequency synthesizer design.

Wes Grammer received the BSEE degree from the University of New Mexico and M.S. Degree in electrical engineering from the University of Massachusetts, then joined Hittite Microwave Corp. Since 1994, he has been employed by the National Radio Astronomy Observatory in, Green Bank, WV.

Peter Katzin received the B.S. degree in physics and electrical engineering from the University of Manchester, England in 1979 and an M.Eng. degree in electrical engineering in 1983 from Cornell University. From 1987 to 1994 he was with Hittite Microwave Corp. He joined Analog Devices Inc. in 1994.